Proceedings of the 9th World Congress on Momentum, Heat and Mass Transfer (MHMT 2024)
London, United Kingdom – April 11 – 13, 2024
Paper No. ICMFHT 126
DOI: 10.11159/icmfht24.126

Exploring Lagrangian Modelling Approach for Nanoparticle Transport in Microchannels

Ahmad Chehade, Anas Alazzam, Eiyad Abu-Nada*
Khalifa University of Science and Technology
Abu Dhabi, UAE
100063093@ku.ac.ae; anas.alazzam@ku.ac.ae
Khalifa University of Science and Technology
Abu Dhabi, UAE
eiyad.abunada@ku.ac.ae

Abstract - In this paper, we introduced a Lagrangian modelling approach to investigate the transport of particles at the nano/micro scale within a microchannel. The methodology of this work involves several stages. Initially, we used Langevin equation and then solved it numerically by finite difference approach to mimic particle transport. Subsequently, we explored various useful macroscopic quantities such as mean square displacement, particle trajectory, and identified numerous timescales of the Brownian motion involved. We considered two fundamental forces, specifically the Brownian force and the hydrodynamic force, with a particular emphasis on the Brownian force. The white noise term and random walk trajectories were solved numerically and simulated for various time step values. Moreover, we explored time scales greater than momentum relaxation time, where the suspended microparticles in a fluid flow exhibited distinctive diffusion behaviour. Furthermore, we observed the suspension of nanoparticles with a low Stokes number ($St \ll 1$) transport in the fluid flow direction. Furthermore, we explored a one-way coupling approach between suspended alumina nanoparticles in a water-based fluid. Lastly, we conducted a detailed validation with previously published work in literature and found a good agreement.

Keywords**:** Lagrangian approach, White noise, Brownian motion, Brownian force, Random Walk

1 INTRODUCTION

The Lagrangian approach establishes a fundamental and crucial concept in the domain of Computational Fluid Dynamics (CFD) and the particular tracking of particles, particularly in the context of microscopic scales [1]. This approach offers a powerful framework for the in-depth investigation of the dynamics displayed by particles suspended within a fluid medium. Within this approach, every individual particle is viewed as a distinct entity surrounded by the surrounding fluid particles, and its motion is tracked over time. The historical importance of this approach started particularly in the context of mixing and transport and have been recognized as crucial back in the 20th century [2]. This has played a key role in understanding particle transport phenomena in microfluidic modelling [3] .Over the last decade, researchers have been exploring this approach for numerous applications, such as the Brownian movement of suspended particles within a fluid medium [4]. Volpe and Giovanni [5] used Lagrangian approach, targeting to enhance the understanding of optically trapped Brownian particles. They developed an algorithm for simulating particle motion, and its motion under the impact of inertial effects. Their work represents a significant step towards unravelling the complexities of stochastic phenomena in this context. Another study examining complex Brownian motion systems was conducted to compare simulation methods based on Einstein-Smoluchowski's theory and Langevin's theory. This research, led by Liu and Jia [6] , they observed that both methods effectively simulate Brownian motion. However, the random walking model was well suited for multiple particles in containers, while Langevin theory was preferable for single particles influenced by external forces. In a related study, Yoshida et al. [7] conducted a study where they simulated the Brownian particles in fluid under influence of hydrodynamic force . In their work, they combined the Langevin equation for particle motion with the lattice Boltzmann method for fluid flow. Another study done by Beysens [8], he conducted a study on the Brownian motion of colloids in liquid mixtures. His work revealed that colloidal motion initially slows due to increased viscosity from concentration fluctuations and shear flow. Nevertheless, the suspended particle size and continuous phase viscosity are crucial factors affecting suspension stability for high levels of particle concentration dispersed within a fluid medium [9]. Brownian motion exhibits an inverse correlation

with fluid viscosity and particle size, especially when particles are in the nanometer range. Additionally, as the fluid's temperature rises, the Brownian motion tends to increase. This irregular motion is due to the continuous collision of the immersed particle with the fluid particle, random density variations in the fluid. Additionally, the mass difference between the immersed particle and fluid particle [10]. Given the multitude of factors influencing Brownian motion, it remains a complex and partly unresolved phenomenon, with some aspects still awaiting further discovery and understanding. The Eulerian approach provides a structured framework for analysing and simulating fluid behaviour within a defined space, focusing on fluid properties at fixed grid points over time and space [11]. However, when dealing with phenomena like Brownian motion at microscopic levels, particularly with low particle concentrations and short time scales [12], the Eulerian modelling approach faces challenges in offering a detailed description of particle diffusion and trajectories under such conditions. This often requires the utilization of alternative modelling methods. Our work aims to enhance our comprehension of Eulerian-Lagrangian coupling approach that can be implemented in such systems that involve a Brownian motion phenomenon. Hence, Eulerian-Lagrangian coupling modelling approach, investigate the interaction between suspended nano/micro particles and the carrier fluid phase. Our objective is to model particle phase dispersion through the utilization of the Lagrangian approach, which enables us to portray particle transport within a base fluid. The Lagrangian approach used in this study is further coupled with an existing in-house Eulerian code. This effort aims to explore the mutual influence of the base fluid and nanoparticle phases, a concept referred to as the two-way coupling approach.

2 METHODOLOGY

2.1 Brownian Motion and Langevin Equation

Brownian motion is a stochastic process responsible for the random movements of microscopic particles suspended within a fluid, whether it exists as a liquid or gas [13]. This random motion is primarily a consequence of the continuous collisions occurring between these microscopic particles and the fluid's surrounding particles [14]. The first observation of this phenomenon dates back to 1827 when Robert Brown noted that pollen grains, suspended in water and viewed under a microscope, exhibited irregular and undirected motions [15].The Brownian motion in conventional fluids depends on several factors, including fluid viscosity, temperature, and particle size [16]. In 1908, Paul Langevin conducted a significant study on the trajectory of a single particle submerged within a fluid and the forces exerted on it within the bulk fluid [17] .He identified two principal forces at play: the drag force and the random force (Brownian force) acting upon suspended particles in a fluid. Fig.1(a) illustrates a large solid particle immersed within a fluid, encircled by fluid molecules in motion, each undergoing random movements. The Langevin equation is an extension of Newton's second law of motion, specifically focusing on two primary forces affecting the immersed particle: the viscous drag force and the Brownian force [18]. Stoke's law applies to the viscous drag force in scenarios characterized by laminar flow with very low Reynolds numbers [19]. The Brownian force arises due to continuous collisions between the immersed particle and fluid particles, as well as random density fluctuations within the fluid. Fig.1(b) provides a visual representation of an immersed particle in a fluid and the concurrent forces. The Langevin equation in terms of particle position is expressed in Eq.(1) , The left-hand side of Eq.(1) represents the inertia term, where m_p signifies the particle's

$$m_p \frac{d^2 x_p}{dt^2} = -\frac{dx_p}{dt}\gamma + \sqrt{2\gamma k_B T}\, W(t) \quad (1)$$

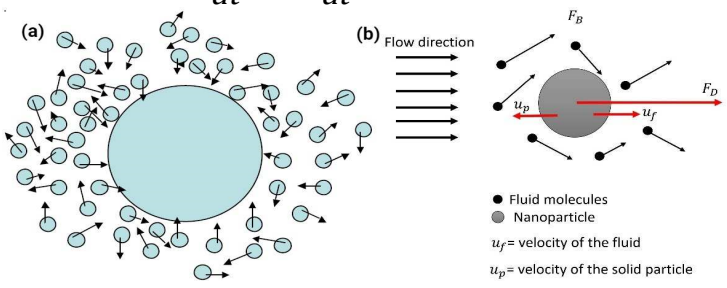

Fig.1.(a) Immersed solid particle in fluid medium: the big particle represents the immersed particle, and the small particles represent the base fluid particles, (b) present forces acting on the immersed particle in a fluid flow.

mass and second term represents its acceleration. Conversely, the right-hand side of Eq.(1) represents the instantaneous forces acting on the suspended particle. In Eq.(1) , the first term on the right side represents the Stokes drag force on a spherical solid particle in a fluid. It is determined by the relative velocity between the particle and fluid, with the second term denoting the Stokes' friction coefficient, $\gamma = 6\pi\mu r$. Here, μ is fluid viscosity, and r is the particle's radius. The negative sign indicates the drag opposes the particle's motion (assuming the fluid is stationary)., The Brownian force, expressed in terms of white noise, where W(t) represents a Gaussian random number with a mean of zero and a variance of $1/\Delta t$ [20]. Here, k_B represents Boltzmann's constant, and T denotes the absolute temperature.

The particle's position at a given time, with respect to random displacement, is presented in Eq.(2) which describes the random walk [21]. Here, w_i represents a Gaussian random number with a mean of zero and a unit variance, it is evident that the immersed particle's position at a specific time relies on its previous position and the random displacement. The path of a microscopic particle within a fluid experiences alterations due to continual collisions between the surrounding fluid molecules and the immersed particles (see Fig.1). Subsequently, these particles disperse throughout the fluid medium, with their speed being impacted by these collisions. Every particle possesses inertia, which governs its behaviour based on its kinetic energy and the influences exerted by the fluid molecules. Einstein proposed the concept of "momentum relaxation time" to describe the timescale of interaction between immersed particles and surrounding fluid molecules (τ_p) [22]. This time scale characterizes the particle's trajectory behaviour as it represents the transition from a ballistic regime to a diffusive regime [23]. It is determined by the ratio of the particle's mass m_p to Stokes' fraction coefficient γ. Initially, the particle's trajectory is smooth as it moves at its own velocity before encountering fluid molecules, constituting a ballistic motion phase. Subsequently, when collisions with fluid molecules commence, the motion shifts to diffusion motion. This resulting motion is described and derived from Langevin's Eq.(1) to account for particle motion influenced by inertia. When particles move in the absence of inertia, where viscous forces surpass inertia forces (assuming $m_p=0$ to eliminate the inertia term in Langevin's equation), the acquired trajectory is presented by Eq.(3) in terms of the diffusion coefficient and white noise. The diffusion coefficient (D) quantifies how quickly a microscopic particle moves randomly within a fluid [24]. It is related to temperature (T), the Boltzmann constant (k_B), and the Stokes' fraction coefficient (γ) through the Stokes-Einstein relation, expressed as $D = k_B T/\gamma$.

$$x(t') = x(t) + \sqrt{\Delta t}\, w(t) \tag{2}$$

$$\dot{x}(t) = \sqrt{2D}\, W(t) \tag{3}$$

Distinguishing and gaining insights into the unrestricted diffusion of immersed particles and the distinction between ballistic and diffusive regimes cannot be determined solely by knowing the particle's position. To address this, a derived statistical metric from the particle's trajectory called the mean square displacement (MSD) is employed. MSD measures how a particle deviates from its reference position over time, representing the average square displacement of all immersed particles at a given time [25]. Einstein introduced the concept of mean square displacement in terms of the particle's diffusion coefficient. According to Einstein's approach, the MSD increases linearly with time and is governed by 2Dt [26] . For time step much smaller than the momentum relaxation time, particles exhibit ballistic movement, with the MSD in this regime governed by $(k_B T/m_p)\, t^2$. Conversely, for $(\Delta t \geq \tau_p)$, it distinctly follows from Einstein's theory that the MSD is proportional to t (diffusive movement). The expression for MSD is presented in Eq.(4).

$$\langle x(t)^2 \rangle = \overline{[x(t+\Delta t) - x(t)]^2} \tag{4}$$

2.2 Discretizing the Lagrangian equation

In our methodology, we start by simulation of Brownian motion by using a white noise, representing Gaussian random numbers with zero mean and a variance of $1/\Delta t$. We thoroughly examined various time step values in relative to the momentum relaxation time to investigate particle transition behaviour. The Lagrangian model equations (Eqs.(1)-(4)) are discretized and solved using the finite difference method (FDM) and Euler's method. The discretizations are given in the following set of equations:

Eq.(5) provides the trajectory of the immersed particle, under the effects of inertia in terms of τ_p and fluid temperature (T_f). The equation representing random movement due to continuous collisions and random displacement is expressed as

Eq.(6). The trajectory of the immersed particle in the absence of inertia is given in Eq.(7). Finally, the Mean Square Displacement (MSD) expression, calculated from the particle position at a given time step, is presented in Eq.(8). This systematic approach allows us to analyse particle transport comprehensively.

$$x_i = \frac{2+\Delta t(\frac{1}{\tau_p})}{1+\Delta t(\frac{1}{\tau_p})} x_{i-1} - \frac{1}{1+\Delta t\left(\frac{1}{\tau_p}\right)} x_{i-2} + \frac{\sqrt{2\gamma k_B T_f}}{m_p\left(1+\Delta t\left(\frac{1}{\tau_p}\right)\right)} w_i \, (\Delta t)^{3/2} \tag{5}$$

$$x_i = x_{i-1} + \sqrt{\Delta t}\, w_i \tag{6}$$

$$x_i = x_{i-1} + \sqrt{2\frac{k_B T \Delta t}{\gamma}}\, w_i \tag{7}$$

$$\langle x_n^2 \rangle = \overline{[x_{i+n} - x_i]^2} \tag{8}$$

3 RESULTS AND DISCUSSION

The generated plots depict W_i values at various time step intervals, specifically Δt = 1, 0.5, and 0.1 seconds. As illustrated in the Fig.2, it becomes evident that Wi values increase as Δt approaches zero and decrease conversely. Furthermore, we can also observe, how the values are distributed around the zero mean. Given that white noise has a variance equal to $1/\Delta t$, the corresponding variances for the three Δt values are 1, 2, and 10, respectively. This leads to a noticeable divergence of W_i values around the zero mean. Consequently, for smaller time step values, the random walk equation is computed with larger white noise values. Solving the random walk Eq.(6) , the numerical solutions become rougher as time step decreases. However, all trajectories showed a similar behaviour around the zero mean. Remarkably, the solution for the smallest Δt results in a more erratic trajectory compared to the others. Fig.3 illustrates the simulation results depicting the trajectories of a particle submerged in a fluid influenced by the inertia terms, Eq.(5). These simulations were conducted using two different time step values, particularly 10 ns and 10 μs, while keeping the momentum relaxation time constant at 0.6 μs. It is important to note that these simulations involved 10,000 trajectories. In Fig.3(a), we can clearly see that when the time step (Δt) is very small compared to the characteristic time (τ_p), the particle's movement is influenced by inertia (as shown by the red solid line). During this regime, the particle undergoes a linear transition with a well-defined velocity, and its position changes smoothly at each time step. In contrast, when inertia is absent (as indicated by the black solid line), the particle's movement appears irregular and discontinuous. In simpler terms, the particles begin to diffusively move in random directions, and the velocity changes unpredictably and abruptly at specific time step values. Moving to Fig.3(b), when Δt is significantly larger than τ_p, both inertial and non-inertial trajectories exhibit similar behaviour. In this scenario, both trajectories appear jagged and discontinuous, reflecting diffusive particle behaviour. The simulation parameters for the spherical silica microparticle are detailed in Table 1. In this context, the subscript 'p' relates to the particle phase, while 'f' refers to the fluid phase.

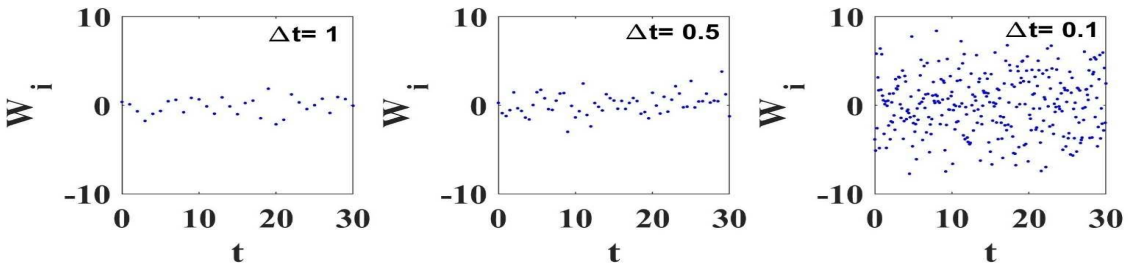

Fig.2.Simulation of white noise term at different time step Δt values.

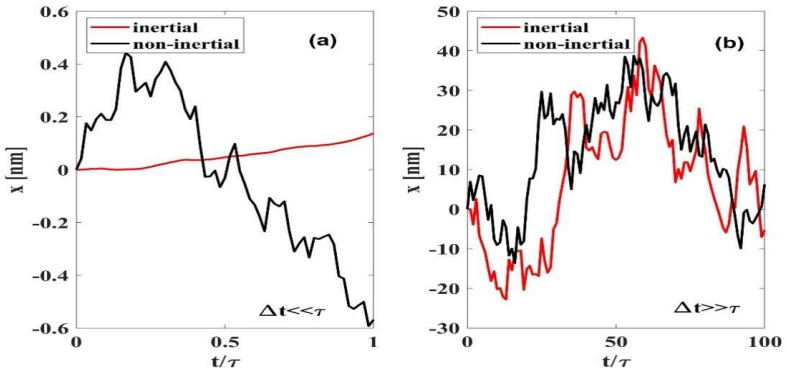

Fig.3. Particle trajectories with different time step values, (a) Δt = 10 ns and (b) Δt = 10 μs

The simulation results of Mean Square Displacement (MSD) are presented in Fig.4 for various time step values, corresponding to intervals of 10 ns, 100 ns, and 10 μs. In Fig.4(a), it is evident that when silica microparticles are subject to inertia (as indicated by the red solid line), they follow a ballistic trajectory. During this phase, the MSD values exhibit a quadratic relationship with time. Conversely, in the absence of inertia, the trajectory transitions into a linear pattern. For time steps exceeding the particle momentum relaxation, as shown in Fig.4(b) and (c), the silica microparticle displays a linear transition for both inertial and non-inertial trajectories. The calculated MSD for silica microparticles immersed in water has been validated compared to Volpe and Giovanni [5] work, demonstrating a good agreement as shown in Fig.4(d).

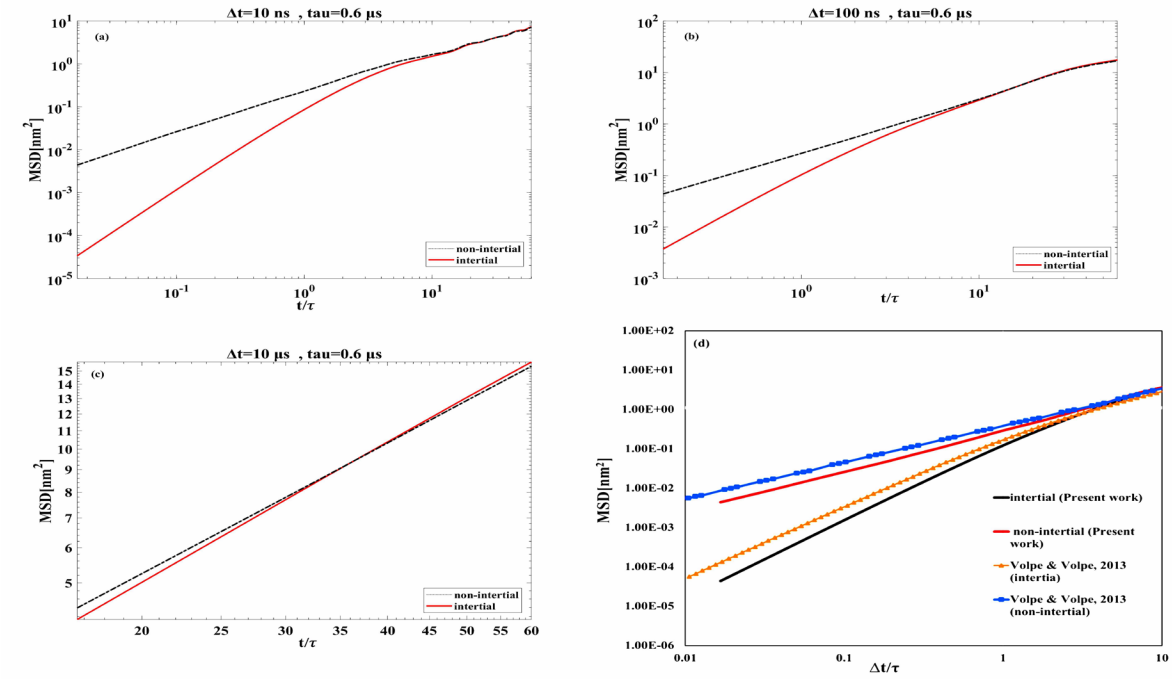

Fig.4.Illustration of Mean Square Displacement (MSD) simulation (a)-(c) for various time step values and (d) validation of the calculated MSD for a silica microparticle submerged in water [5].

Finally, alumina nanoparticles are dispersed at the mid-section of rectangular microchannel, where they experience a transient laminar fluid flow characterized by low Reynolds numbers (Re≤16). The base fluid employed in this study is water, and its thermophysical properties were considered at 298K. In the results we considered a one-way coupling, where the fluid affects the nanoparticles and neglecting the effect of nanoparticles on the base fluid. The base fluid used is water, entering at a velocity of 0.24 m/s. Key simulation parameters can be found in Table 1.Here, 'p' designates the particle phase, while 'f' represents the fluid phase. In Fig.5(a), we observe that the particle moves in alignment with the fluid flow direction. This behaviour arises because the particle's momentum response time (4.057×10^{-10} s) is significantly smaller than that of the fluid (2.52×10^{-4} s). Consequently, the Stokes number, which reflects the ratio of particle momentum response time to characteristic response time of the fluid [27], must be less than one. The governing equation for the Stokes number is represented by Eq.(9) .Here, τ_p denotes the particle response time, and τ_f stands for the characteristic response time of the fluid. However, high Stokes number indicates that particles exhibit more inertia-driven behaviour and are less affected by fluid flow [28].However, the continuum description of the fluid phase is justified based on Knudsen number , in our specific case, stands at a value of 0.001. Consequently, no slip-boundary effects are observed at the interface between the fluid and particle phases. Moreover, given our use of a water-based fluid, the slip velocity becomes almost negligible at the micro-scale. Remarkably, particle velocities closely match fluid velocities at the microchannel's mid-section and at the outlet. Fig.5(b) illustrates the horizontal velocity values at the microchannel's mid-section (x/L=300µm).

$$St = \frac{\tau_p}{\tau_f} \tag{9}$$

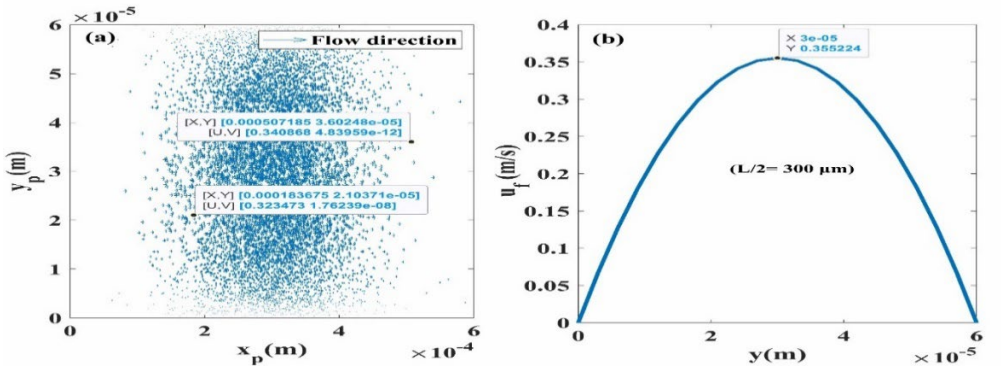

Fig.5.(a) Vector field plot of up and vp in correspondence to particle positions (NP=10000 particles), (b) horizontal velocity at microchannel mid-section (L/2=300µm).

Table 1:Input parameters used in the simulations.

Parameter	Alumina	Silica
Base fluid	Water	Water
Re	16	-
ρ_f(kg m^{-3})	998	998
C_f(J kg^{-1} K^{-1})	4180	4180
T_f (K)	298	300
D_p (nm)	47	0.5
Δt_f (µs)	1	0.6
Δt_p (ns)	1	10
u_o	0.24	-
N_p	10000	-
H(µm)	60	-
L(µm)	600	-

4 CONCLUSION

This work investigated the Lagrangian modelling approach to gain insights into nano- and micro-sized spherical particle transport within microchannels. Our methodology used the Langevin equation and was solved numerically using a finite difference scheme. Remarkably, we observed that as the time step value decreased, the white noise term's value increased, resulting in jagged particle trajectories and an immediate transition to diffusion. Concerning MSD, we observed that particles exhibited a ballistic transition for time steps smaller than the momentum relaxation time, shifting to a diffusive transition for time steps larger than the momentum relaxation time. Additionally, in a one-way coupling between suspended alumina nanoparticles and the fluid phase, we noted that particle velocities at different locations closely matched the outlet velocity of the fluid phase. Looking forward, our research will continue to evolve. We plan to incorporate considerations for momentum and thermal exchange between the fluid and particle phases by using a two-way coupling approach, with a particular focus on investigating convective heat transfer enhancements. These future aims to significantly contribute to our understanding of nanoparticle transport in microchannels.

References

[1] M. Sommerfeld, Y. Cui, and S. Schmalfuß, "Potential and constraints for the application of CFD combined with Lagrangian particle tracking to dry powder inhalers," *Eur. J. Pharm. Sci.*, vol. 128, no. December 2018, pp. 299–324, 2019, doi: 10.1016/j.ejps.2018.12.008.

[2] E. van Sebille, S. M. Griffies, R. Abernathey, and Adams, "Lagrangian ocean analysis: Fundamentals and practices," *Ocean Model.*, vol. 121, no. November 2017, pp. 49–75, 2018, doi: 10.1016/j.ocemod.2017.11.008.

[3] Y. Won and J. Yul, "Transport of solid particles in microfluidic channels," *Opt. Lasers Eng.*, vol. 50, no. 1, pp. 87–98, 2012, doi: 10.1016/j.optlaseng.2011.06.027.

[4] Y. Yang and B. Li, "A simulation algorithm for Brownian dynamics on complex curved surfaces," *J. Chem. Phys.*, vol. 151, no. 16, pp. 1–28, 2019, doi: 10.1063/1.5126201.

[5] G. Volpe and G. Volpe, "Simulation of a Brownian particle in an optical trap," *Am. J. Phys.*, vol. 81, no. 3, pp. 224–230, Mar. 2013, doi: 10.1119/1.4772632.

[6] Z. Liu and Y. Jia, "Two simulation methods of Brownian motion," *J. Phys. Conf. Ser.*, vol. 2012, no. 1, 2021, doi: 10.1088/1742-6596/2012/1/012015.

[7] H. Yoshida, T. Kinjo, and H. Washizu, "Numerical simulation method for Brownian particles dispersed in incompressible fluids," *Chem. Phys. Lett.*, vol. 737, no. September, p. 136809, 2019, doi: 10.1016/j.cplett.2019.136809.

[8] D. Beysens, "Brownian motion in strongly fluctuating liquid," *HAL open Sci.*, pp. 1–8, 2023, [Online]. Available: https://hal.science/hal-04005221/document

[9] M. M. El-Tonsy, A. H. Oraby, and W. T. F. Al-Ibraheemi, "Physical Characterization of a Method for Production of High Stability Suspension," *Int. J. Sci. Eng. Appl.*, vol. 5, no. 2, pp. 42–60, 2016, doi: 10.7753/ijsea0502.1001.

[10] A. Norouzipour, A. Abdollahi, and M. Afrand, "Experimental study of the optimum size of silica nanoparticles on the pool boiling heat transfer coefficient of silicon oxide/deionized water nanofluid," *Powder Technol.*, vol. 345, pp. 728–738, Mar. 2019, doi: 10.1016/j.powtec.2019.01.034.

[11] M. S. Shadloo, G. Oger, and D. Le Touzé, "Smoothed particle hydrodynamics method for fluid flows, towards industrial applications: Motivations, Current state, And challenges," *Comput. Fluids*, vol. 136, no. June 2016, pp. 11–34, 2016, doi: 10.1016/j.compfluid.2016.05.029.

[12] M. S. Saidi, M. Rismanian, M. Monjezi, M. Zendehbad, and S. Fatehiboroujeni, "Comparison between Lagrangian and Eulerian approaches in predicting motion of micron-sized particles in laminar flows," *Atmos. Environ.*, vol. 89, pp. 199–206, 2014, doi: 10.1016/j.atmosenv.2014.01.069.

[13] P. H. Jones, O. M. Maragò, and G. Volpe, "Brownian motion," in *Optical Tweezers*, Cambridge University Press, 2015, pp. 188–218. doi: 10.1017/cbo9781107279711.009.

[14] J. Mo and M. G. Raizen, "Highly Resolved Brownian Motion in Space and in Time," *Annu. Rev. Fluid Mech*, vol. 51, pp. 403–428, 2019, doi: 10.1146/annurev-fluid-010518.

[15] M. Pancorbo, M. A. Rubio, and P. Domínguez-García, "Brownian dynamics simulations to explore experimental microsphere diffusion with optical tweezers," in *Procedia Computer Science*, Elsevier B.V., 2017, pp. 166–174. doi: 10.1016/j.procs.2017.05.231.

[16] T. Li and M. G. Raizen, "Brownian motion at short time scales," *Ann. Phys.*, vol. 525, no. 4, pp. 281–295, 2013, doi:

10.1002/andp.201200232.
[17] J. Mo and M. G. Raizen, “Highly Resolved Brownian Motion in Space and in Time,” *Annu. Rev. Fluid Mech.*, 2019, doi: https://doi.org/10.1146/annurev-fluid-010518-040527.
[18] A. Genthon, “The concept of velocity in the history of Brownian motion: From physics to mathematics and back,” *Eur. Phys. J. H*, vol. 45, no. 1, pp. 49–105, Jul. 2020, doi: 10.1140/epjh/e2020-10009-8.
[19] R. Huang, I. Chavez, and K. M. Taute, “Direct observation of the full transition from ballistic to diffusive Brownian motion in a liquid,” *Nat. Phys.*, vol. 7, no. 7, pp. 576–580, 2011, doi: 10.1038/nphys1953.
[20] S. Sharma and Vishwamittar, “Brownian motion problem: Random walk and beyond,” *Resonance*, vol. 10, no. 8, pp. 49–66, 2005, doi: 10.1007/bf02866746.
[21] P. Hurtado, “Computational Methods in Nonlinear Physics 4. Stochastic Processes and Stochastic Differential Equations,” Cambridge University Press, 2014.
[22] S. Dong, L. Zheng, X. Zhang, S. Wu, and B. Shen, “A new model for Brownian force and the application to simulating nanofluid flow,” *Microfluid. Nanofluidics*, vol. 16, no. 1–2, pp. 131–139, 2014, doi: 10.1007/s10404-013-1213-x.
[23] B. S. Der and B. Kuhlman, “From computational design to a protein that binds,” *Science*, vol. 332, no. 6031. pp. 801–802, May 13, 2011. doi: 10.1126/science.1207082.
[24] J. Spiechowicz, I. G. Marchenko, P. Hänggi, and J. Łuczka, “Diffusion Coefficient of a Brownian Particle in Equilibrium and Nonequilibrium: Einstein Model and Beyond,” *Entropy*, vol. 25, no. 1, pp. 1–25, 2023, doi: 10.3390/e25010042.
[25] M. K. Riahi, I. A. Qattan, J. Hassan, and D. Homouz, “Identifying short- and long-time modes of the mean-square displacement: An improved nonlinear fitting approach,” *AIP Adv.*, vol. 9, no. 5, 2019, doi: 10.1063/1.5098051.
[26] R. Huang, B. Lukic, S. Jeney, and E.-L. Florin, “Direct observation of ballistic Brownian motion on a single particle,” no. March, 2010, [Online]. Available: http://arxiv.org/abs/1003.1980
[27] B. Wang and M. Manhart, “Two-phase micro- and macro-time scales in particle-laden turbulent channel flows,” *Acta Mech. Sin. Xuebao*, vol. 28, no. 3, pp. 595–604, 2012, doi: 10.1007/s10409-012-0034-6.
[28] J. Mollicone, M. Sharifi, F. Battista, P. Gualtieri, and C. M. Casciola, “Particles in turbulent separated flow over a bump : Effect of the Stokes number and lift force Particles in turbulent separated flow over a bump : Effect of the Stokes number and lift force,” vol. 103305, no. October, 2019, doi: 10.1063/1.5119103.